

Liquefaction mitigation using 3D printed geocells

Prerana Krishnaraj¹, Gali Madhavi Latha², and T. G. Sitharam³

¹Research Scholar, Indian Institute of Science, Bangalore, India, email: preranak@iisc.ac.in

²Professor, Indian Institute of Science, Bangalore, India, email: madhavi@iisc.ac.in

³Professor, Indian Institute of Science, Bangalore, India, email: sitharam@iisc.ac.in

ABSTRACT

Mitigation of liquefaction through conventional techniques like densification, grouting, and earthquake drains are well-explored in the literature. However, the use of geosynthetics for liquefaction mitigation has not emerged as a popular solution because of the lack of fundamental research in this direction and practical difficulties in reinforcing the ground beneath foundations and other structures. In this context, the present study proposes geocells for liquefaction mitigation, which can be easily adopted in the construction of retaining walls, slopes, and bridge abutments. The basic principle of strength improvement through geocells is the increase in the confinement of the soils, which is beneficial for liquefaction mitigation. The higher confinement has multiple benefits, including densification, development of apparent cohesion, and an increase in frictional strength, which hampers soil liquefaction. Cyclic triaxial tests are conducted on geocell reinforced sands to understand these aspects. These geocells are indigenously manufactured in our laboratory through 3D printing of polymeric sheets and ultrasonic welding. 3D printing is especially useful in creating specific geocells with controlled dimensions, scaled tensile strength, and desired surface features. These geocells are filled with saturated sand and tested under sinusoidal loading. The effects of printing parameters on the pore water pressure development in specimens are studied. Results are analysed to bring out the quantitative benefits of geocell reinforcement in reducing the excess pore water pressure and increasing the number of cycles required for liquefaction.

Keywords: Soil liquefaction, geocell, cyclic triaxial test, 3D printing

1 INTRODUCTION

Loose saturated sand deposits tend to densify under the action of monotonic or cyclic loadings. In undrained conditions, the tendency to densify causes the pore water pressure to increase causing the effective stress to decrease. This phenomenon is termed liquefaction. The catastrophic damages caused to the liquefaction during the Niigata earthquake and Alaska earthquake in 1964 led to extensive liquefaction-related studies.

The liquefaction mitigation techniques are mainly classified as soil densification, soil reinforcement, degree of saturation reduction and drainage techniques (Huang & Wen, 2015). The soil reinforcement techniques mainly involve reinforcing soil with stone columns, metal strips or geosynthetics. Over the last three decades, rigorous research has been carried out to understand the effects of geosynthetic reinforcements in planar and fiber forms on the liquefaction response of the sand.

Krishnaswamy and Isaac (1994) conducted stress controlled triaxial tests on reinforced sand and suggested that there is an increase in the effective confining pressure due to the inclusion of the geosynthetics leading to the reduction in liquefaction potential. This reduction in liquefaction potential was found to be more pronounced at lower relative densities and with the use of geosynthetics having higher stiffness and interface friction properties. Vercueil et.al (1997) found that the inclusion of the compressible non-woven geotextile layers improved the liquefaction resistance of the sand. Boominathan and Hari (2002) found a significant improvement in the liquefaction resistance of the fly ash reinforced with fiber elements and mesh elements through a series of cyclic triaxial tests. Altun et.al (2008) conducted cyclic torsional shear tests and found that the liquefaction resistance of the sand reinforced with non-woven geotextiles was higher than that reinforced with woven geotextiles. Ibraim et.al (2010) and Liu et.al (2011) studied the static liquefaction behaviour of the sand samples reinforced

with flexible fibers through undrained triaxial tests and ring-shear tests respectively. Ye et.al (2017) studied the effects of randomly distributed polypropylene fibres on liquefaction response through undrained cyclic triaxial tests and found that the liquefaction resistance increased with the fibre content and fibre length.

3D printing is the process of manufacturing material using 3D model data, one layer at a time (Campbell et al.,2011). Initially, 3D sketch of the model to be printed is drawn using any appropriate software. The drawing is further converted into an STL (Stereolithography language) file (Wong & Hernandez, 2012). The printer will print one layer at a time to form the required model. The Fused Deposition Method (FDM) based printers are mostly used for 3D printing of the polymeric components (Vaezi et al.,2013). It works on extrusion principle where the extruded material is deposited on the flat base to form a 2D layer deposition one over the other to form a 3D object. In this technique, the filaments of the thermoplastics are melted and extruded through the heated nozzle.

3D printing can provide a very efficient and time saving method for obtaining geocell material of desired strength characteristics. If the sensitivity and relation of various printing parameters with respect to the strength and friction characteristics of the fabricated material are established, it can be a very useful technique to aid model testing of geosynthetic reinforced geomaterials.

The liquefaction response of the geocell reinforced saturated sand under dynamic loading has not been explored. In this study, geocells manufactured from 3D printing of polypropylene sheets, which are further ultrasonically welded were used to reinforce the sand. The strain-controlled cyclic triaxial tests were conducted on both the unreinforced and geocell reinforced samples. The performance of the geocell reinforced sand samples were found to be superior to that of unreinforced sand samples. Further, the effects of various printing parameters on the improvement in liquefaction resistance were also studied.

2 MATERIALS

2.1 Sand

The cyclic triaxial tests were conducted on the river sand from the Cauvery River basin, Karnataka, India. Figure 1 gives the particle size distribution curve of the sand used. The properties of the sand used in this study are given in Table 1. According to the Unified Soil Classification System (USCS), this sand is classified as poorly graded(SP).

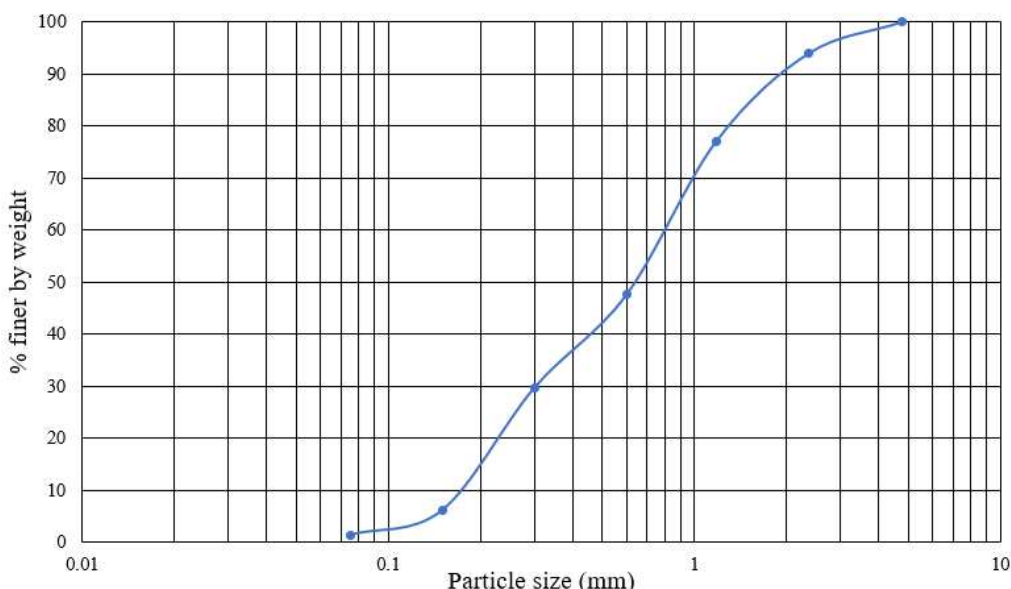


Figure 1. Particle size distribution of the river sand used in the study

Table 1. Properties of the sand

| Properties | Values |
|---|--------|
| Specific gravity | 2.63 |
| Effective particle size (D_{10}) (mm) | 0.175 |
| D_{30} (mm) | 0.305 |
| D_{50} (mm) | 0.648 |
| D_{60} (mm) | 0.844 |
| C_u | 4.823 |
| C_c | 0.630 |
| e_{max} | 0.897 |
| e_{min} | 0.43 |

2.2 Geocells

The study has been carried out using geocells that are 3D printed and ultrasonically welded. The Fused Deposition Method (FDM) based 3D printer was used for the study. The 3D printer used in this study is shown in Figure 2. The 3D printing of the polypropylene sheets was carried out under different conditions of the angle of printing, speed of printing, and the number of layers of printing. Polypropylene sheets of thickness 0.4 mm have been used for all the analyses. Figure 3 shows the three different configurations of the angle of printing used in the study. Table 2 gives the nomenclature that will be followed in this paper.

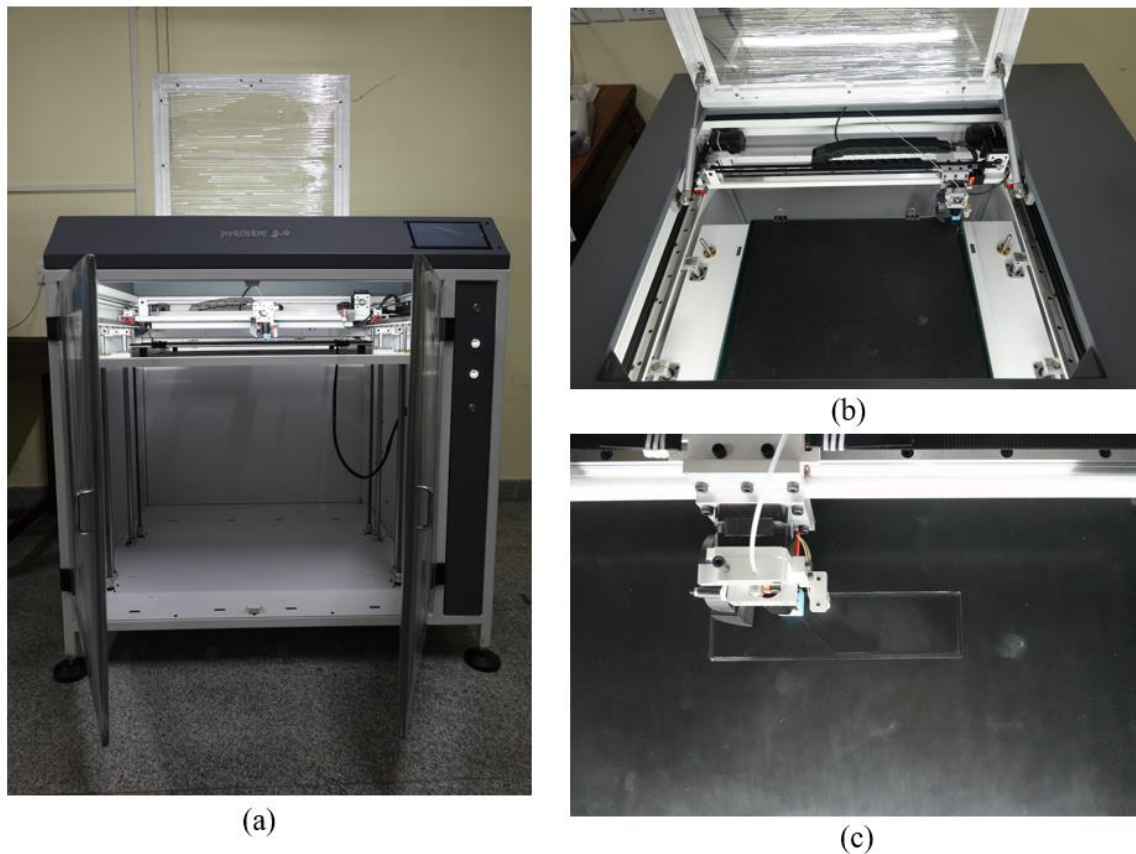


Figure 2. (a) Front view of the 3D printer (b) Printing bed (c) Printing of polypropylene sheet

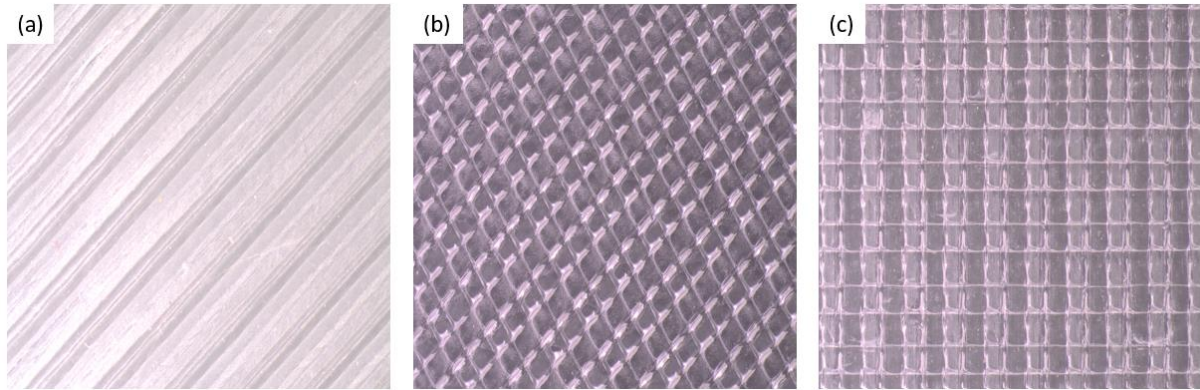


Figure 3. (a) Single layered sheet printed at 45° angle (b) Two-layered sheet printed at 45° angle (c) Two-layered sheet printed at 0° angle

Table 2. Nomenclature used in the study

| Nomenclature | Angle of printing(°) | Speed of printing (mm/s) | Number of printing layers |
|--------------|----------------------|--------------------------|---------------------------|
| A45S30L1 | 45 | 30 | 1 |
| A45S30L2 | 45 | 30 | 2 |
| A45S40L2 | 45 | 40 | 2 |
| A0S30L2 | 0 | 30 | 2 |

The 3D-printed polypropylene sheets were then ultrasonically welded at regular intervals, which when expanded form a honeycomb-shaped structure. The welding time was selected in such a way that the peel strength of the weld was greater than 0.9 times the ultimate tensile strength of the polypropylene sheet.

3 CYCLIC TRIAXIAL TESTS

The strain-controlled triaxial tests were conducted on the samples of diameter 70 mm and height 140 mm. The samples were prepared using the wet pluviation technique. This technique helps in achieving the uniform density of the sample in addition to closely representing the natural sand deposition process. A relative density of 30% was maintained for both the unreinforced and geocell reinforced samples. This represents the relative density before the consolidation process. The sample preparation was carried out in number of trials to ensure the uniform relative density in all the tests. The relative density of the sample was calculated based on the maximum void ratio and minimum void ratio of the sand mentioned in the Table 1. The relative density of 30% corresponds to a void ratio of 0.76. Many researchers have found that liquefaction predominantly occurs in saturated loose cohesionless soils. Since this study focuses on the mitigation of the liquefaction using geocells, a relative density of 30% which represents loose soil deposits have been considered. In the geocell reinforced case, geocell of equivalent diameter 60 mm was placed in the cell and the wet pluviation was carried out as shown in the Figure 4. The cohesion and friction angle of the unreinforced and geocell reinforced sand were obtained through static triaxial tests. The cohesion and friction angle of the unreinforced and geocell reinforced were 0 kPa and 34.5°, and 29.6 kPa and 33.1°, respectively. Figure 5 shows the cylindrical sample of diameter 70 mm and height 140 mm, and the triaxial cell mounted on the loading frame.

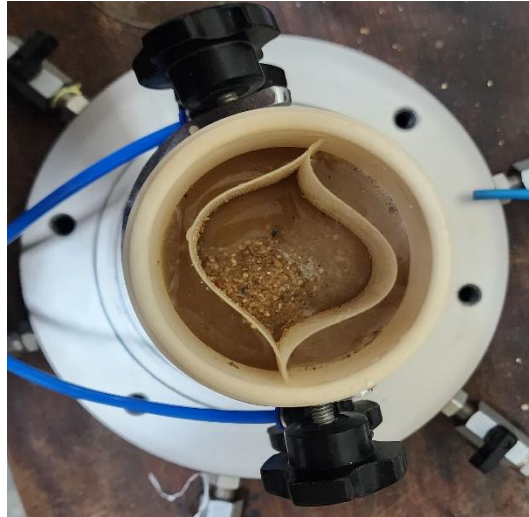


Figure 4. Triaxial test sample with geocell

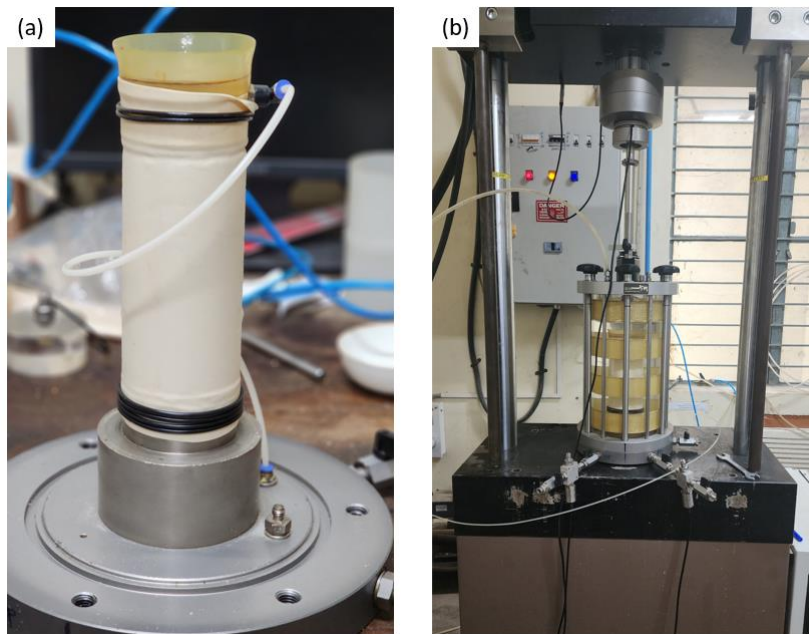


Figure 5. (a) Cylindrical sample of diameter 70 mm (b) Triaxial cell mounted on the loading frame

After mounting the sample on the loading frame, the sample was saturated. The sample was considered to be fully saturated when the value of Skempton's parameter B was equal to or greater than 0.99. The value of B was calculated as the ratio of the increase in the pore water pressure to the increase in the confining stress. The saturated sample was then consolidated to an effective confining stress of 200 kPa. All the tests were conducted at an effective confining pressure of 200 kPa. A sinusoidal loading of single amplitude of 0.5% and frequency of 1 Hz was applied to the top of the consolidated saturated sample. Under undrained conditions, the pore water pressure increases with number of cycles due to the contractive nature of the sample. The variation of the pore water pressure ratio with the number of cycles was plotted. The pore water pressure ratio is defined as the ratio of the excess pore water pressure developed to the initial effective confining pressure. The sample was considered to be liquefied when the value of the pore water pressure ratio becomes greater than 0.98.

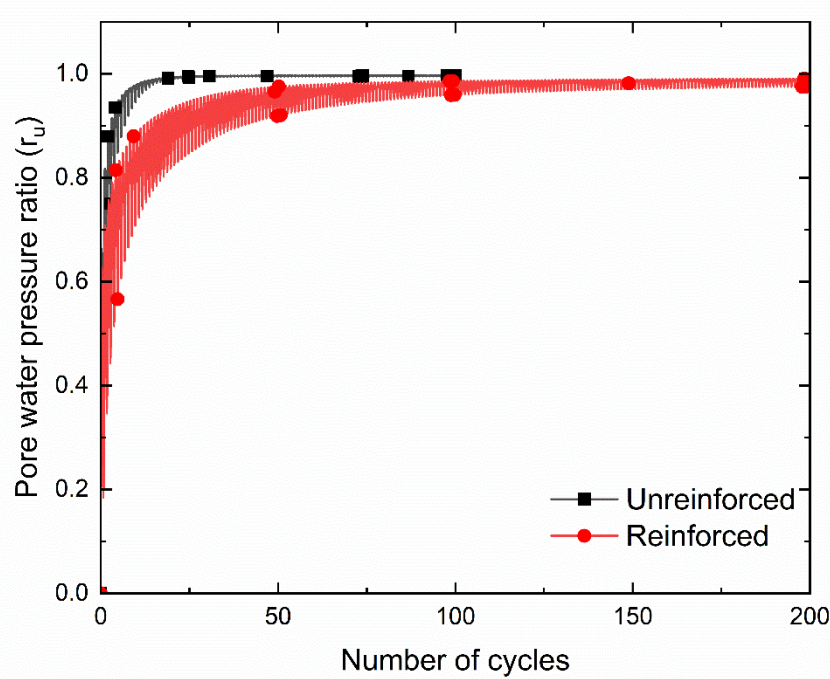


Figure 6. Variation of the pore water pressure ratio with number of cycles for unreinforced and geocell reinforced sand samples

From Figure 6, it can be seen that the unreinforced sand sample liquefies around the twelfth cycle, whereas in the reinforced sand sample, the number of cycles of loading required for the sample to liquefy increased substantially indicating the beneficial effects of the inclusion of the geocell reinforcement.

4 RESULTS AND DISCUSSIONS

A series of cyclic triaxial tests were conducted on the geocell reinforced sand samples to understand the effects of various printing parameters on the liquefaction resistance. The effects of angle of printing, number of layers of printing and speed of printing on the number of cycles required for the sand to liquefy was studied.

4.1 Effects of angle of printing

Two layered polypropylene sheets printed at a speed of 30 mm/s were considered. The angles of printing of 45° and 0° were considered for the analyses. Figure 7 gives the variation of the excess pore water pressure with number of cycles of loading. It is seen that for the sand reinforced with geocells printed at an angle of 45°, the number cycles of loading required for the sand sample to liquefy was around 61 whereas it was around 129 cycles for the angle of printing of 0°. The narrow-width tensile tests conducted on the reinforcement samples indicated that the ultimate tensile strength of the sheets printed at an angle of 45° and 0° was 5.75 kN/m and 5.7 kN/m respectively.

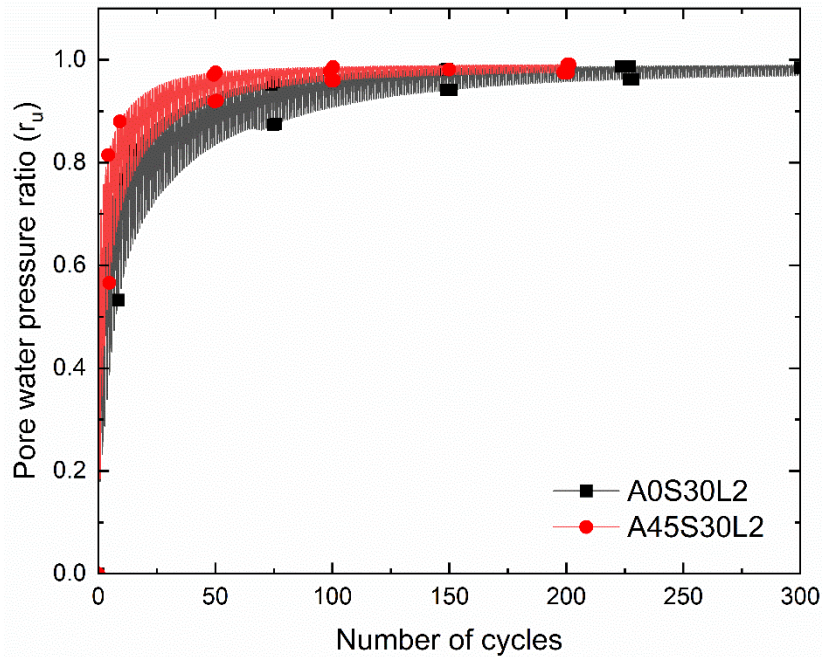


Figure 7. Variation of the pore water pressure ratio with the number of cycles for different angles of printing

4.2 Effects of the number of layers of printing

Experiments were carried out on the sand samples reinforced with geocells printed at an angle of 45° and a speed of 30 mm/s. The sheets printed as a single layer of thickness 0.4 mm and two layers, each of thickness 0.2 mm were considered. For two layered sheets, the angles of printing were considered as +45° and -45°. The variation of the pore water pressure ratio with the number of cycles of loading is shown in Figure 8. The number of cycles of loading required for the reinforced sample to liquefy was around 42 for single layered geocell sheet and around 61 cycles for 2 layered geocell sheet. The results from the narrow-width tensile tests showed that the ultimate tensile strength of the single-layered and double layered sheet was 2.9 kN/m and 5.75 kN/m respectively.

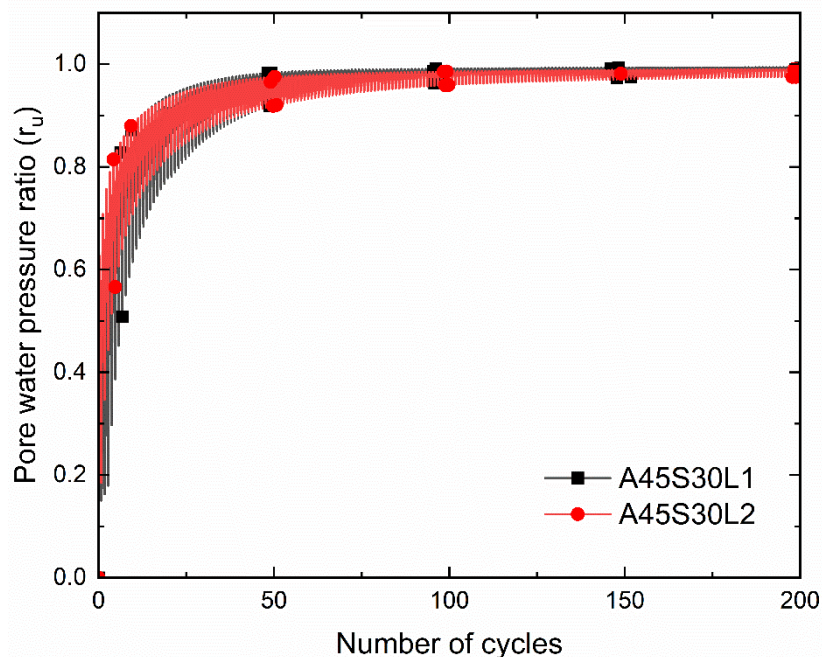


Figure 8. Variation of the pore water pressure ratio with number of cycles for single layered and two layered polypropylene sheet

4.3 Effects of the speed of printing

Two layered sheets printed at an angle of 45° and at the printing speeds of 30 mm/s and 40 mm/s were considered in the study. From Figure 9, it can be seen that the difference in the pore water pressure ratio developed for both cases is not significant. But the number of cycles required for the reinforced sample to liquefy was found to be around 61 cycles for the speed of printing of 30 mm/s and around 49 cycles for the speed of printing of 40 mm/s. From the narrow-width tensile tests, it was seen that the ultimate tensile strength of the sheets printed at different speeds was almost the same.

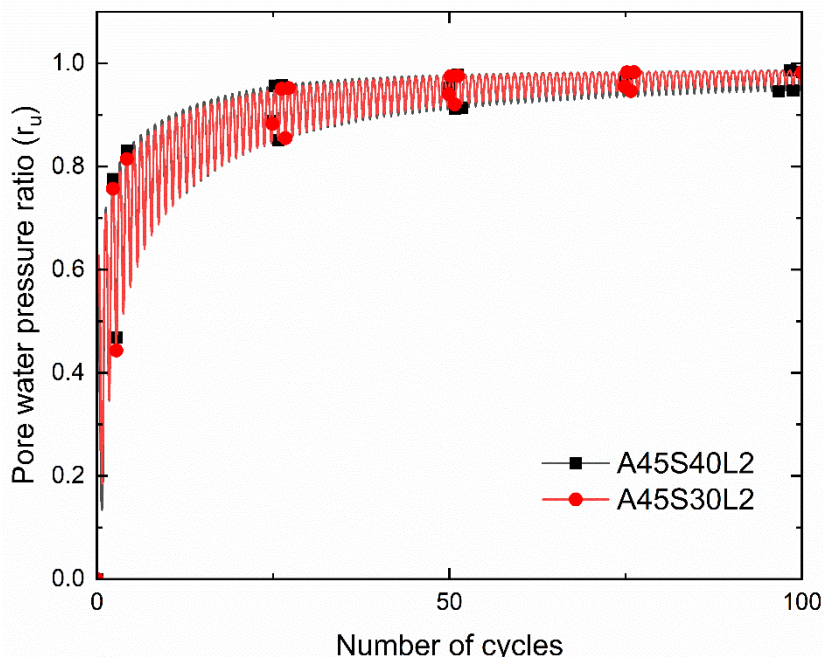


Figure 9. Variation of the pore water pressure ratio with number of cycles for different speeds of printing

Table 3. summarises the number of cycles required for the sand samples to liquefy for unreinforced and different geocell reinforced cases. Further, the values of Young's modulus of the sample for all the cases were calculated. It is seen that there is a substantial improvement in both Young's modulus as well liquefaction resistance of the sand due to the inclusion of the geocell reinforcement.

Table 3. Results from cyclic triaxial tests

| Nomenclature | Number of cycles required to liquefy | Young's modulus (MPa) |
|--------------|--------------------------------------|-----------------------|
| Unreinforced | 12 | 31.8 |
| A45S30L1 | 42 | 34.8 |
| A45S30L2 | 61 | 38.8 |
| A45S40L2 | 49 | 38.5 |
| A0S30L2 | 128 | 38.6 |

5 CONCLUSIONS

The effects of the speed of printing, the angle of printing, and the number of layers of printing on the liquefaction response of the geocell reinforced sand were studied through cyclic triaxial tests.

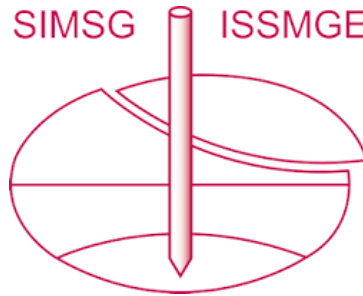
- The number of cycles required for the reinforced sand sample to liquefy was found to depend significantly on the angle of printing.
- Liquefaction resistance of the sand reinforced with geocell obtained from double layered polypropylene sheet was higher than that reinforced with geocell obtained from single layered polypropylene sheet.
- The speed of printing was found to have the least effect on the liquefaction response of the reinforced sample as compared to the angle of printing and number of layers of printing.

- The results showed that there is a substantial increase in the liquefaction resistance of the sand due to the inclusion of the geocell reinforcement indicating that the geocell reinforcement can be used as a liquefaction mitigation technique in areas susceptible to liquefaction.

REFERENCES

- Altun, S., Göktepe, A. B., & Lav, M. A. (2008). Liquefaction resistance of sand reinforced with geosynthetics. *Geosynthetics International*, 15(5), 322-332.
- Boominathan, A., & Hari, S. (2002). Liquefaction strength of fly ash reinforced with randomly distributed fibers. *Soil Dynamics and Earthquake Engineering*, 22(9-12), 1027-1033.
- Campbell, T. (2011). Could 3D printing change the world?: Technologies, potential, and implications of additive manufacturing.
- Huang, Y., & Wen, Z. (2015). Recent developments of soil improvement methods for seismic liquefaction mitigation. *Natural Hazards*, 76, 1927-1938.
- Ibraim, E., Diambra, A., Wood, D. M., & Russell, A. R. (2010). Static liquefaction of fibre reinforced sand under monotonic loading. *Geotextiles and Geomembranes*, 28(4), 374-385.
- Krishnaswamy, N. R., & Isaac, N. T. (1994). Liquefaction potential of reinforced sand. *Geotextiles and Geomembranes*, 13(1), 23-41.
- Liu, J., Wang, G., Kamai, T., Zhang, F., Yang, J., & Shi, B. (2011). Static liquefaction behavior of saturated fiber-reinforced sand in undrained ring-shear tests. *Geotextiles and Geomembranes*, 29(5), 462-471.
- Vaezi, M., Seitz, H., & Yang, S. (2013). A review on 3D micro-additive manufacturing technologies. *The International Journal of Advanced Manufacturing Technology*, 67, 1721-1754.
- Vercueil, D., Billet, P., & Cordary, D. (1997). Study of the liquefaction resistance of a saturated sand reinforced with geosynthetics. *Soil Dynamics and Earthquake Engineering*, 16(7-8), 417-425.
- Wong, K. V., & Hernandez, A. (2012). A review of additive manufacturing. *International scholarly research notices*, 2012.
- Ye, B., Cheng, Z. R., Liu, C., Zhang, Y. D., & Lu, P. (2017). Liquefaction resistance of sand reinforced with randomly distributed polypropylene fibres. *Geosynthetics International*, 24(6), 625-636.

INTERNATIONAL SOCIETY FOR SOIL MECHANICS AND GEOTECHNICAL ENGINEERING



This paper was downloaded from the Online Library of the International Society for Soil Mechanics and Geotechnical Engineering (ISSMGE). The library is available here:

<https://www.issmge.org/publications/online-library>

This is an open-access database that archives thousands of papers published under the Auspices of the ISSMGE and maintained by the Innovation and Development Committee of ISSMGE.

The paper was published in the proceedings of the 9th International Congress on Environmental Geotechnics (9ICEG), Volume 5, and was edited by Tugce Baser, Arvin Farid, Xunchang Fei and Dimitrios Zekkos. The conference was held from June 25th to June 28th 2023 in Chania, Crete, Greece.